W and Z physics at the Fermilab Tevatron

P. Pétroff

LAL 07-188
November 2007

W and Z Physics at the Fermilab Tevatron

Pierre Pétroff
LAL, Univ Paris-Sud, CNRS/IN2P3, Orsay, France

Talk given at the XXIII International Symposium on Lepton and Photon Interactions at High Energy ("**LP07**"**)**
Daegu, Korea, August 13-18, 2007

U.M.R
de
l'Université Paris-Sud

Institut National de
Physique Nucléaire et de
Physique des Particules du CNRS

LAL ~ Bât. 200 ~ B.P. 34 ~ 91898 Orsay Cedex ~ France

LAL 07-188
November 2007

W and Z Physics at the Fermilab Tevatron

Pierre Pétroff

LAL, Univ Paris-Sud, CNRS/IN2P3, Orsay, France

Abstract

Electroweak measurements performed by CDF and DØ are reported, corresponding to data collected at the center-of-mass energy of 1.96 TeV with a luminosity ranging from 0.2 fb^{-1} to 2 fb^{-1}. The current status and future prospects for high precision measurements of electroweak parameters and detailed studies of boson production are highlighted.

1 Introduction

The study of the electroweak gauge bosons W and Z is an important part of the physics programs at the Tevatron. Their large production rates and clean experimental signatures in leptonic decay modes facilitate several important measurements, such as the determination of the electroweak parameters M_W and Γ_W and the extraction of the parton distribution functions of the proton. The diboson production processes based on clean and well understood signatures are robust tests of the Standard Model (SM) and allow exploration beyond the SM scenarios.

Due to a large QCD background, decay channels involving quarks are difficult to measure; therefore W and Z bosons are mainly identified through their leptonic decays. These decays are characterized by a high transverse energy lepton $p_T(l)$ and large transverse missing energy $\not\!\!E_T$for W, or by two high transverse energy leptons for Z.

Electrons are identified as an electromagnetic (EM) cluster using a simple cone algorithm. To reduce the background of jets faking electrons, electron candidates are required to have a large fraction of their energy deposited in the EM section of the calorimeter and pass energy isolation and shower shape requirements. The weak bosons backgrounds and the signal have been estimated using a Monte Carlo simulation. Electron candidates are classified as *tight* if a track is matched spatially to EM cluster and if the track transverse momentum is close to the transverse energy of the EM cluster. In CDF, electrons are reconstructed both in the central calorimeter and plug calorimeter ($|\eta| < 2.8$)[1] while electrons in DØ are reconstructed in the central and endcaps calorimeters ($|\eta| < 1$ and $1.5 < |\eta| < 3.2$). Both CDF and DØ require at least one *tight* electron in the central calorimeter ($|\eta| < 1$) for $Z \to e^+e^-$ candidates.

Muons are identified by a track in the muon system matched to a track in the central tracking system. For CDF the measurement in the muon channel includes the muons reconstructed in the central muon extension sub-detector which extends the coverage from $|\eta| < 0.6$ to $|\eta| < 1$. For DØ the muon reconstruction is extended to the forward muon detector with a coverage up to $|\eta| = 2.0$.

Muons from the decay of heavy-flavor hadrons are significant background to vector bosons production. It can be reduced by requiring that the muon is isolated. Cosmic ray muons contaminate the muon sample. Timing capabilities and distance of the muon track to the vertex are used to reduce the cosmic rays muons background to low level.

[1] $\eta = -\ln\tan(\theta/2$, where θ is the polar angle with respect to the proton direction

2 Studies of Boson Production

2.1 $Z \to \tau\tau$ cross section

The CDF and DØ collaborations have published a measurement of the Z boson production in the $\tau\tau$ decay channel with 0.35 fb^{-1} [1] and 0.23 fb^{-1} [2] data sample, respectively. More recently, DØ has performed a measurement with an integrated luminosity of 1.0 fb^{-1} in the channel in which one τ decays into $\mu\nu_\mu\nu_\tau$ and the other into hadrons+ν_τ or $e\nu_e\nu_\tau$. The total efficiency for $Z \to \tau^+\tau^-$ events in the 60-130 GeV mass region is 4.89 10^{-3}. The result, $\sigma(p\overline{p} \to Z)BR(Z \to \tau^+\tau^-) = 237 \pm 8(stat) \pm 13(sys) \pm 15(lumi)$ pb,
is in good agreement with the standard model NNLO prediction [3] using either the MRST2004 NNLO parton density functions or CTEQ6.1M NNLO PDF parametrizations. Figure 1 shows a comparison of this result with all other Z cross section measurements performed at CDF and DØ as well as the theoretical calculation from [3]. This demonstrate the ability at Tevatron to identify and reconstruct tau leptons and thus establish the sensitivity for observing signatures such as $H \to \tau\tau$.

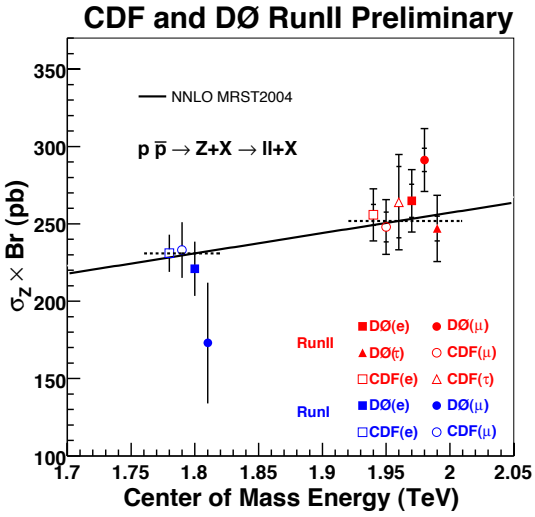

Figure 1: *Comparison of the available mesured Z cross section times branching ratio performed by CDF and DØ in all lepton channels to the theoretical prediction of [3]*

2.2 $d\sigma/dy$ distributions of Drell-Yan dielectron pairs

Measurement of the differential boson production cross section over the full rapidity range provide stringent constraints on PDF parametrizations. The dilepton decay modes of the Z boson allow for precise measurements, since backgrounds in these final states are small, and the full event kinematics can be precisely reconstructed.
At leading order Z/γ^* bosons are produced through the annihilation of a quark and an anti-quark, with the partons in the proton and anti-proton carrying momentum fractions x_1 and x_2, respectively. The rapidity of the boson, defined as $y = \frac{1}{2}\ln\frac{E+p_L}{E-p_L}$, where E is the energy of the boson and p_L is its longitudinal component, is directly related to the momentum fractions by $x_{1,1} = \frac{M_{Z/\gamma^*}}{\sqrt{s}}\exp^{\pm y}$
Here, M_{Z/γ^*} is the mass of the boson, and $\sqrt{s}$ is the center of mass energy.
The forward rapidity region $|y| > 1.5$ probes quarks with low x and high 4-momentum transfer squared Q^2 ($Q^2 \approx M_Z^2$) as well as quarks with very large x. Both CDF and DØ measured the differential cross section distribution $1/\sigma\frac{d\sigma}{dy}$, using dielectrons from Z/γ^* decays.

Figure 2 shows the rapidity distribution using 0.4 fb^{-1} [4] in the DØ experiment The curve is a NNLO calculation from Ref.[5] generated with MRST 2004 NNLO PDFs [6]. The calculation agrees well with the data.

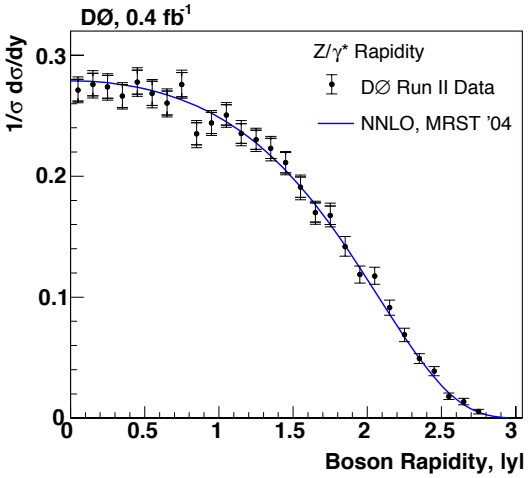

Figure 2: *DØ Run II measurement of $1/\sigma d\sigma/dy$. The inner (outer) bars show the statistical (total) uncertainty. The curve is a NNLO calculation from [5] using MRST 2004 PDFs.*

More recently, CDF has measured the $d\sigma/dy$ cross section with an integrated luminosity of 1.1 fb^{-1}. The total cross section from integrating $d\sigma/dy$ is

$\sigma = 263.34 \pm 0.93(stat) \pm 3.79(syst)$. The luminosity error of 6% is not included in the systematic error. The NLO calculation with NLO CTEQ6.1 PDF [7] is the most consistent with the data.
Figure 3 shows a comparison with theory. A deviation at 1 σ level from present PDFs at high x is observed.

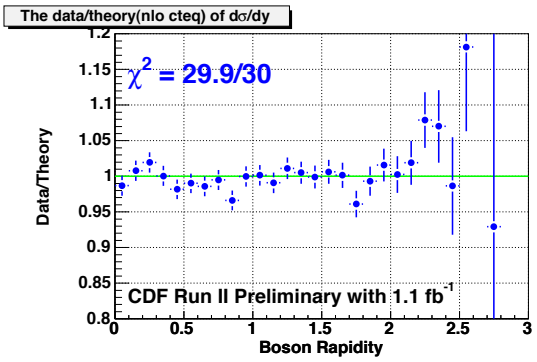

Figure 3: *CDF Run II measurement of the ratio of the data to the theory prediction with NLO calculation and with NLO CTEQ6.1 PDFs*

2.3 Z boson transverse momentum study

Z boson production serves as an ideal testing ground for predictions of quantum chromodynamics (QCD) at higher order calculations. The boson's transverse momentum, q_T, can be measured over a wide range of values and can be correlated with its rapidity. At high q_T (> 20 GeV), the radiation of a single parton with large transverse momentum dominates the cross section, and one expects perturbative QCD at NNLO [8] to yield reliable predictions. To cope with multiple soft gluon emission at lower q_T, a soft gluon emission resummation technique has been developed by Collins, Soper and Sterman (CSS) [9].
Z boson q_T distributions have been published previously by CDF [10] and DØ [11]using about 100 pb^{-1} of data. More recently DØ has reported a new measurement with 0.98 fb^{-1}. This measurement is the first to present a q_T distribution for forward-rapidity Z bosons.
Figure 4 shows the measured differential cross section in the range $0 < q_T < 260$ GeV/c. The ResBos+PHOTOS prediction [12, 13] describes the data well for $q_T < 30$ GeV/c but underestimates the cross section at high q_T. The NNLO [8] prediction describes the data well for $q_T > 30$ GeV/c.

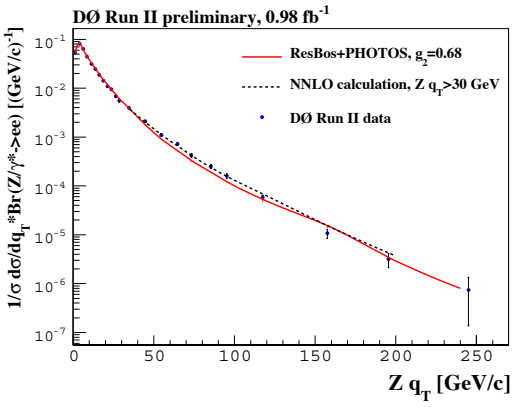

Figure 4: *DØ measurement of the differential cross section as function of q_T compared to the theoretical calculations (see text for more details).*

2.4 W boson charge asymmetry

Direct Measurement of W boson charge asymmetry provides new input on the momentum fraction dependence of the u and d quark parton distribution function (PDF) within the proton.
As the u quark tends to carry a higher fraction of the proton's momentum than the d quark, the $W^+(W^-)$ is boosted, on average, in the proton(anti-proton) direction.
The $W^\pm$ charge asymmetry is defined as

$$A(y_W) = \frac{d\sigma(W^+)/dy_W - d\sigma(W^-)/dy_W}{d\sigma(W^+/dy_W) + d\sigma(W^-)/dy_W}$$

Measurements are typically performed using the charged leptons (e or μ) for the W boson decays. Since the longitudinal momentum of the neutrino is unmeasured, the asymmetry has been measured traditionally [15] as

$$A(\eta_e) = \frac{d\sigma(e^+)/d\sigma\eta_e - d\sigma(e^-)/d\sigma\eta_e}{d\sigma(e^+)/d\sigma\eta_e + d\sigma(e^-)/d\sigma\eta_e}$$

where η_e is the electron pseudo-rapidity. The lepton asymmetry, $A(\eta_e)$ is the convolution of $W^\pm$ production and V-A (vector-axial vector) decay asymmetries.
A new DØ measurement [16] of the lepton charge asymmetry using $W \to \mu\nu$ from 0.3 fb^{-1} data sample is shown in Fig. 5. Charge misidentification rate is one of the major key experimental issues. DØ measured an average the charge misidentification probability of $0.00005^{+0.00012}_{-0.0000087}$ out to $\eta_\mu = 2$. The measured asymmetry is compared to

a theoretical prediction based on CTEQ6.1M PDF model. The results can already improve constraints on PDFs, especially for $0.7 < |\eta_\mu| < 1.3$.

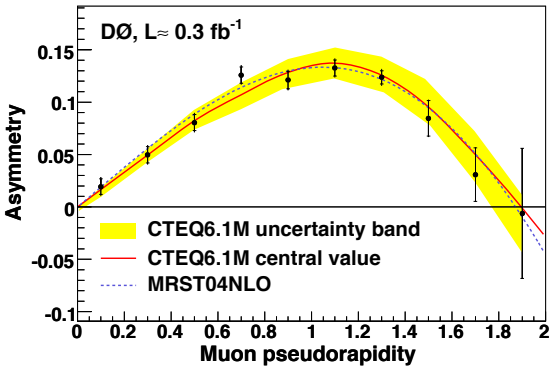

Figure 5: *DØ folded muon charge asymmetry distribution. The shaded (yellow) band is the envelope determined using forty CTEQ6.1M PDF uncertainty sets, the solid (red) line is the CTEQ6.1M central value, and the dotted (blue) line is the charge asymmetry determined using MRST04 NLO PDFs.*

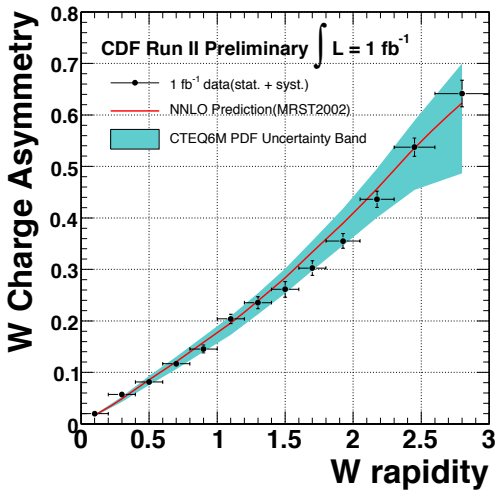

Figure 6: *CDF direct measured asymmetry, $A|y_W|$ with prediction from CTEQ5L. The band curves are from the variation of 20 pairs of independent PDF parameters and illustrate the range of uncertainty on CTEQ prediction.*

CDF has presented a new analysis method that reconstruct the W rapidity from $W \rightarrow e\nu$ data using an integrated luminosity of 1.0 fb^{-1}. This method fully exploits the kinematic information in W events to directly reconstruct the underlying W boson production asymmetry. The W boson rapidity is ambiguous since the longitudinal momentum of the neutrino from its decay cannot be measured. However the neutrino momentum can be determined to a two-fold ambiguity by constraining the W mass.This ambiguity can be partly solved on a statistical basis from the known V-A decay distribution and the $W^{\pm}$ production cross section as a function of y_W and $d\sigma/dy$.
Figure 6 summarizes the results compared to an NNLO prediction [17] using MRST2002 PDFs [18] and CTEQ5L PDFs with the corresponding errors PDFs from CTEQ6.1 described by 20 parameters [19].
The CDF direct asymmetry measurement method indicates the possibility of a significant increase in sensitivity.

2.5 Direct Measurement of the Z boson invisible width

CDF has performed a direct measurement of the Z boson invisible width $\Gamma(Z \rightarrow inv)$ from an analysis of events with large $\not\!\!E_T$and one or more energetic jets. The originally purpose of this analysis was a search of new physics. However, in the observed absence of a data excess over the Standard Model (SM) expectation, CDF has interpreted the result in the context of a direct measurement of Z boson invisible width.
This measurement is based on 1 fb^{-1} of data. The data-driven background to new physics search estimates is used excluding the $Z \rightarrow \nu\nu$ channel.
$\Gamma(Z \rightarrow inv) =$
$\frac{\sigma(Z+1-jet)\times Br(Z\rightarrow inv)}{\sigma(Z+1-jet)\times Br(\rightarrow l^+l^-)} \times \Gamma(l^+l^-)$
The PDG value for $\Gamma(l^+l^-)$ (width of Z boson to leptons) is used and the ratio
$\frac{\sigma(Z+1-jet)\times Br(Z\rightarrow inv)}{\sigma(Z+1-jet)\times Br(\rightarrow l^+l^-)}$
is experimentally measured.
Finally CDF measured $\Gamma(Z \rightarrow inv) = (466 \pm 42)$ MeV in good agreement with the combined LEP direct measurement (503 ± 16 MeV) and with an error comparable to that each LEP experiments [22].

3 Dibosons Production Studies

3.1 Introduction

The self-interactions of the gauge boson are a direct result of the non-abelian $SU(2)_L \otimes U(1)_Y$ structure

of the Standard Model (SM). The SM predicts the structure of the correspondant trilinear gauge couplings (TGC). Non-SM particles that couple to the electroweak bosons can modify the expected cross sections, particularly at large transverse momenta of the gauge bosons.
The results from the Tevatron are complementary to those from LEP, since the Tevatron probes different combinations of TGCs at higher $\hat{s}$, where new physics might manifest itself.
CDF and DØ experiments have produced a wide variety of new Run II results based on the study of diboson final states.

3.2 Wγ Production

Wγ production can occur via the WWγ vertex or by the radiation of a photon in the initial or final states. Anomalous WWγ coupling leads to an enhancement in the production cross section and to the rates for events with a high E_T photon or a high transverse mass of the Wγ system.
Both CDF [23] and DØ [24] have measured the Wγ cross section using the leptonic decays of the W boson. New preliminary results with higher statistics, $\approx$ 1 fb^{-1}, are now available. The signature of the Wγ signal is an isolated high p_T lepton, an isolated high $E_T(\gamma)$ photon, and a large $\not\!\!E_T$from the W neutrino.
The photon is required to be well-separated from the lepton. The two analyses require $E_T(\gamma) > 7$ GeV and isolation between the photon and the lepton $\Delta R(l,\gamma)^2 > 0.7$. In addition, DØ requires that the transverse mass $M_T(l\gamma,\nu)$ of the lepton, photon, and neutrino is greater than 90 GeV.

DØ measures, using 0.9 fb^{-1},
$\sigma(p\overline{p} \to \mu\nu\gamma X) =$
$3.21 \pm 0.49(stat+syst) \pm 0.20(lumi)$ pb,
$\sigma(p\overline{p} \to e\nu\gamma X) =$
$3.12 \pm 0.49(stat+syst) \pm 0.19(lumi)$ pb,
compared to a theoretical expectation of
$\sigma(p\overline{p} \to l\nu\gamma X) = 3.21 \pm 0.08$ pb Theory. [25]
CDF measures, using 1.0 fb^{-1},
$\sigma(p\overline{p} \to \mu\nu\gamma X) =$
$19.11 \pm 1.04(stat) \pm 2.40(syst) \pm 1.11(lumi)$ pb,
$\sigma(p\overline{p} \to e\nu\gamma X) =$
$17.21 \pm 0.83(stat) \pm 2.24(syst) \pm 1.00(lumi)$ pb,
compared to a theoretical expectation of
$\sigma(p\overline{p} \to l\nu\gamma X) = 19.3 \pm 1.4$ pb Theory. [25]
The measured cross sections are in good agreement with SM predictions.

[2] $\Delta R(l,\gamma) = \sqrt{(\eta_l - \eta_\gamma)^2 + (\phi_l - \phi_\gamma)^2}$

The kinematic distributions of the candidate events are in agreement with the SM too. Figure 7 shows the photon $E_T(\gamma)$ distribution from CDF as an example.

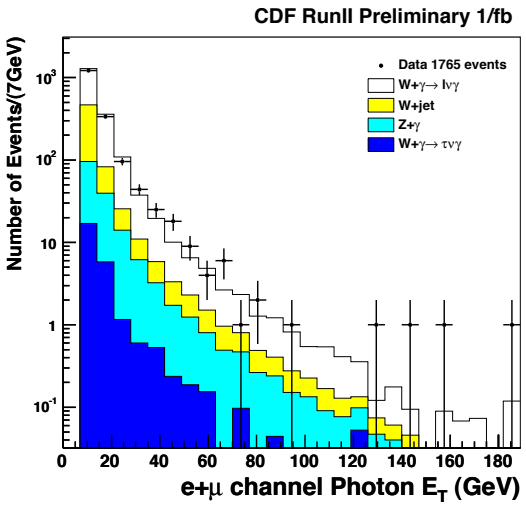

Figure 7: *CDF: Photon $E_T(\gamma)$ distribution of $W(\to l\nu)\gamma$ candidate events*

DØ has performed a study of the charge-signed rapidity difference $Q \times \Delta\eta$, where Q is the charge of the lepton and $\Delta\eta = \eta(\gamma) - \eta(l)$ is the rapidity difference between the photon and the lepton. Figure 8 shows the distribution of this quantity in background-subtracted data, along with the expectation from a Monte Carlo simulation. In the absence of final state radiation and detector effects, the amplitude is expected to be zero at $Q \times \Delta\eta = 0$ due to the "radiation amplitude zero " effect [25]. As expected the dip is somewhat washed out due to the final state radiation and detector resolution effects. The data are in good agreement with SM. For illustration, an alternative MC prediction based on one particular assumption on anomalous coupling (a choice that leads to zero magnetic dipole moment of the W boson) is also shown in Fig. 8. This technique appears very sensitive to anomalous couplings determination.

3.3 Zγ Production

At tree level, a Z boson cannot couple to a photon, *i.e.* the vertices ZZγ and Z$\gamma\gamma$ are forbidden. In the SM, the Zγ final state can, however, be produced by final state radiation (FSR) off both charged leptons from $Z/\gamma \to l^+l^-$ or by one of the partons

in the p or $\overline{p}$ through initial state radiation (ISR). Various extension of the SM [26] predict large anomalous values of the trilinear couplings ZZγ and Z$\gamma\gamma$ that results in an excess of photons with high transverse energy, $E_T(\gamma)$, compared with the SM prediction. An observation of either an enhancement of the cross section or an excess of photons with high $E_T(\gamma)$ would indicate new physics [27].

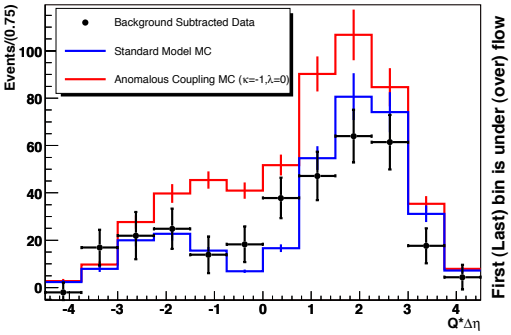

Figure 8: *D0: Comparison of the SM distribution and an anomalous coupling distribution to the background-subtracted charge-signed rapidity difference from data*

Previous studies of Zγ production have been performed at Tevatron by CDF [23] and DØ [28] and at LEP [29]. All results are consistent with SM predictions.
Both CDF and DØ have measured the cross section for Zγ production in datasets of 1 fb^{-1} per experiment. In the CDF analysis, the $Z/\gamma^* \rightarrow e^+e^-$ channel is used while DØ consider both electron and muon channels for the Z decay. Both experiments require the photon to be central ($|\eta| < 1.1$) with $E_T(\gamma) > 7$ GeV and well separated from leptons ($\Delta R(l,\gamma) > 0.7$. Figure 9 shows the distribution of the candidate events from CDF analysis in the
M(e^+e^-)/M($e^+e^-\gamma$) plane. The different production processes like FSR, ISR and Drell-Yan lead to distinctive patterns in the distributions.
CDF and DØ measure cross sections for different cuts on M(e^+e^-) and M($e^+e^-\gamma$).

Requiring M($ee\gamma$) > 40 GeV CDF measured a cross section $\sigma(p\overline{p} \rightarrow Z)BF(Z \rightarrow \ell\ell) = 4.9 \pm 0.3(stat) \pm 0.3(syst) \pm 0.3(lumi)$ pb in good agreement with the theoretical prediction of $4.7 \pm 0.4(syst)$ pb [30]. Very recently, DØ has measured [31] a cross section $\sigma(p\overline{p} \rightarrow Z)BF(Z \rightarrow \ell\ell) = 4.9 \pm 0.3(stat + syst) \pm 0.3(lumi)$ pb with a cut $M(ee) > 30$ GeV. This result is in good agreement too with the theoretical prediction [30], $4.74 \pm 0.22(syst)$ pb. The measured photon E_T spectrum from DØ in Fig. 10 shows a good agreement with the theoretical prediction.

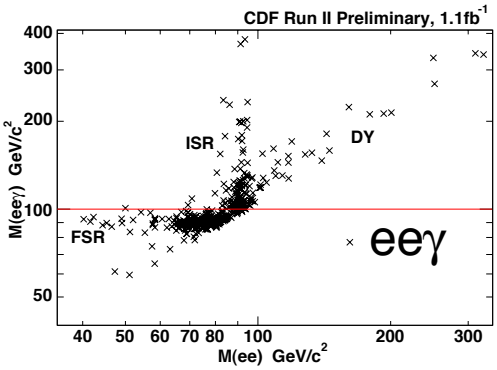

Figure 9: *CDF: Distribution in the $M(e^+e^-)/M(e^+e^-\gamma)$ plane of the Zγ candidates*

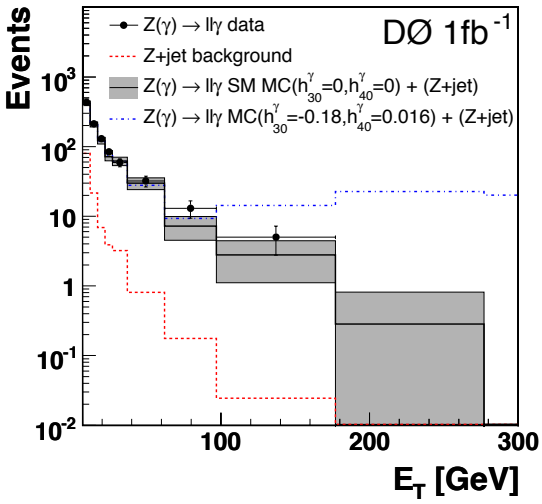

Figure 10: *Photon E_T distribution of DØ Zγ candidates events. SM predictions and predictions from an anomalous coupling model (normalised to luminosity) are also shown. The shaded bands illustrate the statistical and systematics uncertainties on the SM Monte Carlo and Z+jet background prediction.*

DØ [31] has searched for anomalous trilinear ZVγ (V = Z, γ) couplings in the framework of Ref.[32]. Such ZVγ couplings can be parametrized by two CP-violating (h_1^V and h_2^V) and two CP-conserving (h_3^V and h_4^V) complex parameters. Unitarity is en-

sured by using a form factor (Λ) parametrization that causes the coupling to vanish at high center-of-mass energy $\sqrt{\hat{s}}$ [3].
The one dimensional limits at 95% C.L. for CP-conserving couplings are $-0.085 < h_{30}^{\gamma} < 0.084$, $-0.0053 < h_{40}^{\gamma} < 0.0054$ and $-0.083 < h_{30}^{Z} < 0.082$, $-0.0053 < h_{40}^{Z} < -.0054$ for $\Lambda = 1.2$ TeV. DØ expects the limits on CP-violating couplings to be approximately the same. These new limits represent a significant improvment over previous results and the limits on h_{40}^{V} are the most stringent to date.

3.4 WW Production

Production of WW pairs involves both WWγ and WWZ couplings. This channel is an important background in searches for a high-mass Higgs in $H \to WW^*$.
The signature of the WW signal is leptonic decay in two high p_T leptons with opposite charge and large $\not\!\!E_T$from the W neutrinos.
the WW signal in Run II is well established. The measured cross section are
$\sigma(p\overline{p} \to W^+W^-) = 13.6 \pm 2.3(stat) \pm 1.6(syst) \pm 1.2(lumi)$ pb for CDF [33], with 0.825 fb^{-1} and
$\sigma(p\overline{p} \to W^+W^-) = 14.6^{+1.8}_{-3.0}(stat)^{+3.0}_{-1.8}(syst)$
$\pm$ 0.9$(lumi)$ pb for DØ [34], with 0.224-0.252 fb^{-1}.
These results are in good agreement with cross section predicted at next-to-leading order [35].

3.5 Observation of WZ Production

The study of WZ production allows one to search for anomalous WWZ coupling independently of the WWγ coupling, in contrast to WW production. The WZ production has not been conclusively observed up to now.
CDF and DØ use clean $WZ \to l'\nu l^+l^-$ modes. A pair of isolated high p_T leptons consistent with the Z mass is required, plus a third high p_T lepton and missing transverse energy.
In both experiments, all three lepton candidates must pass lepton identification requirement based on the calorimeters and the muon detectors. In order to increase the statistics, the CDF analysis also considers candidate events where up to two candidate leptons are reconstructed only as isolated central tracks that are not fiducial to calorimeters or muon detectors. CDF has published [36] the first observation of the WZ production with 1.1 fb^{-1} data sample. Sixteen WZ candidates are observed with an expected background of 2.7 ± 0.4 events. The signal significance corresponds to 6σ. More recently CDF improved the WZ analysis with a 1.9 fb^{-1} data sample. The preliminary cross section is $\sigma(p\overline{p} \to WZ) = 4.3^{+1.3}_{-1.0}(stat.) \pm 0.2(syst.) \pm 0.3(lumi.)$ pb consistent with the SM expectation [35] 3.68 ± 0.25 pb. Figure 11 shows the final candidate events plotted as a function of $\not\!\!E_T$, along with the expected signal and background contributions.

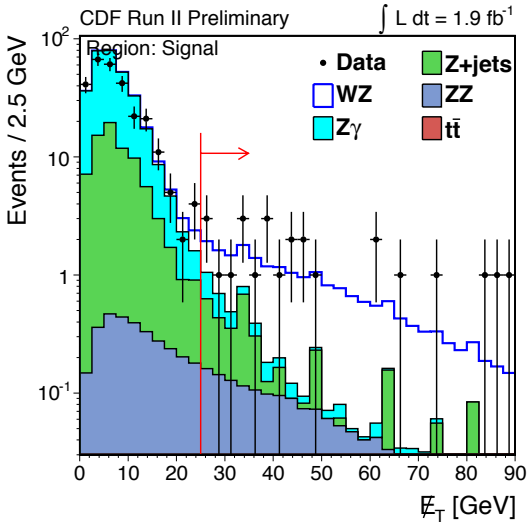

Figure 11: *Comparison of $\not\!\!E_T$ distribution for observed data events with the combined expectation from signal and background in the CDF WZ analysis. The arrow on the figure indicates the signal region for this search (missing $E_T > 25$ GeV).*

DØ observes 13 candidates in a 0.76-0.86 fb^{-1} data sample with an expected background of 4.5 ± 0.6 events. The signal significance corresponds to 3.3σ. The measured cross section, $\sigma(p\overline{p} \to WZ) = 2.7^{+1.3}_{-1.7}$ pb, is in agreement too with the predicted cross section [35].
Both CDF and DØ have interpreted their results in term of limits on anomalous WWZ couplings. The WWZ interaction can be parametrized by a generalized effective Lagrangian [37, 38] with CP-conserving trilinear gauge coupling parameteres (TGCs) g_1^Z , κ_Z and λ_Z that describe the coupling strengths of the vector boson to the weak field. The anomalous TGCs are presented as deviations from their SM values, *i.e.* as $\Delta g_1^Z = g_1^Z$, $\Delta\kappa_Z - 1$, and λ_Z, where $\lambda_Z = 0$ in the SM. Like in the ZZγ/ZZZ analysis a cut-off Λ is used in order to prevent that

[3] $h_i^V = \frac{h_{i0}^V}{(1+\sqrt{\hat{s}}/\Lambda^2)^n}$. h_{i0}^V are the low-energy approximation of the couplings, n is the form-factor power. In accordance with [32], $n = 3$ for $h_{1,3}^V$ and $n = 4$ for $h_{2,4}^V$.

the added terms in the Lagrangian violate unitarity [4]

Because the Tevatron is the only accelerator that can produce the charged state WZ+X, this measurement provide a unique opportunity to study WWZ TGCs without any assumption on the values of WWγ couplings.This is in contrast to WW production in which both WWZ and WWγ TGCs contribute [39].

Both CDF and DØ have performed a preliminary analysis to set anomalous coupling limits. Table 1 presents the one-dimensional 95% C.L. limits on λ_Z, Δg_1^Z and $\Delta\kappa_Z$ from DØ [40]. These limits have been calculated for two sets of form factor scale Λ = 1.5 TeV and 2.0 TeV with 1 fb^{-1} of data.

$\Lambda = 1.5$ TeV	$\Lambda = 2.9$ TeV
$-0.18 < \lambda_Z < 0.22$	$-0.17 < \lambda_Z < 0.21$
$-0.15 < \Delta g_1^Z < 0.35$	$-0.14 < \Delta g_1^Z < 0.34$
$-0.14 < \Delta\kappa_Z < 0.31$	$-0.12 < \Delta\kappa_Z < 0.29$

Table 1: *One-dimensional 95% C.L. intervals on λ_Z, Δg_1^Z, and $\Delta\kappa_Z$ for two sets of form factor scale, Λ. the limits in 3^{rd} row assume that $\Delta\kappa_Z = \Delta g_1^Z$*

CDF obtained the following preliminary limits with 1.9 fb^{-1} of data for Λ = 2. TeV: $-0.13 < \lambda_Z < 0.14$, $-0.15 < \Delta g_1^Z < 0.24$ and, $-0.82 < \Delta\kappa_Z < 1.27$.

These limits will be improved significantly with larger data samples.

3.6 Evidence of ZZ Production

The SM does not predict any self-coupling of Z boson, *i.e.*, the vertices ZZγ and ZZZ are forbidden. The NLO predicted [35] cross section, including one-loop corrections is 1.40 ± 0.1 pb. DØ has reported a search for ZZ production based on 1.0 fb^{-1} while CDF has reported an observation of ZZ production based on 1.5 fb^{-1}

Both CDF and DØ use the clean leptonic $eeee$, $ee\mu\mu$ and $\mu\mu\mu\mu$ channels. CDF has performed a new complementary search in the $l^+l^-\nu\nu$ final states. In that search, contributions from the different modes (WW, ZZ) that contribute to this final state are disentangled using event probabilities calculated from all measured kinematic information and leading order differential cross sections. The results are combined and a binned maximum likelihood fit is performed which contains one bin for the $llll$ channel and 5 bins for $ll\nu\nu$ channels as shown in Fig. 12. The preliminary result is a first 3 σ evidence of ZZ production at a hadron collider. The mesured cross section is $\sigma(p\overline{p} \to ZZ) = 0.75^{+0.71}_{-0.64}$ pb. This results is consistent with SM expectation [35].

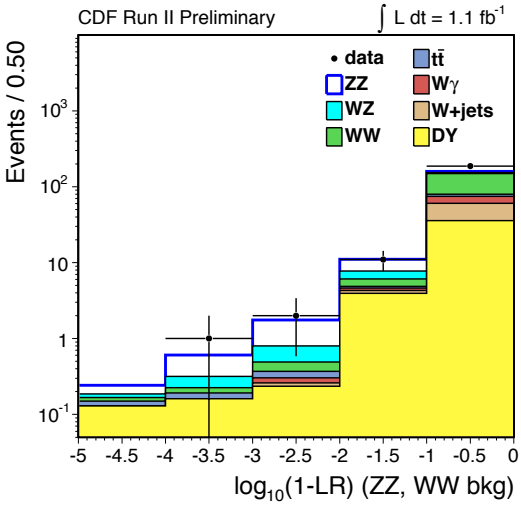

Figure 12: *Distribution of $log_{10}(1-LR)$ used in the fit, LR(Likelihood Ratio) = $\frac{P_{ZZ}}{P_{ZZ}+P_{WW}}$*

4 W mass and width Measurements

4.1 W Boson Mass Measurement

A precision measurement of the W boson mass is of the highest priority for the Tevatron experiments. The W boson mass, combined with precise measurement of the top quark mass (M_{top}), constrains the mass of the Higgs boson. Self-energy corrections to the W boson depend on the masses of the top quark ($\propto M_{top}^2$) and the Higgs boson ($\propto \ln M_H$), as well as potential contributions from non-SM physics [43, 44].

The combined CDF and DØ result [45] on the top quark mass is 170.91 ± 1.8 GeV. The uncertainty corresponds to roughly a 1.1% measurement of M_{top}. For equal contribution to the Higgs boson mass uncertainty, The W boson mass would need to be measured to about 0.014% corresponding to a total uncertainty of 11 MeV.

CDF has reported the first W mass measurement from Run II of the Tevatron collider run. The mass is measured using the electron and muons decay of

[4] $\lambda_Z(\hat{s}) = \lambda_Z/(1+\hat{s}/\Lambda^2)^2$. Where $\hat{s}$ is the sqare of the invariant mass of the WZ system.

the W boson, by fitting the transverse mass [5] and the lepton and neutrino transverse momentum distributions.
In order to select W boson data with low background and well-understood charged lepton and neutrino kinematics, charged lepton p_T and $\not\!\!E_T$ are required to be greater than 30 GeV, and recoil energy in the calorimeter is required to be less than 15 GeV.
The data correspond to 218.1 ± 12.4 pb^{-1} for the electron channel and 190.8 ± 10.9 pb^{-1} for the muon channel.
A sophisticated parametrized Monte Carlo simulation is used to predict the shape of the transverse mass distribution as well as the lepton and neutrino p_T distributions as a function of M_W. The W boson mass is extracted by fitting the M_W prediction of the Monte Carlo simulation to the data with a binned maximum-likelihood fit.
The lineshape predictions depend on a number of physical and detector effects, which can be constrained either from control samples or calculation. Important physical effects include internal QED radiation, the intrinsic W boson transverse momentum, and the proton parton distribution functions (PDF). External bremsstrahlung and ionization energy in the detector material, tracker momentum scale, calorimeter scale, resolutions of the tracker and calorimeter, and the detector fiducial acceptance are among the most important detector effects.
The most important steps of the W mass measurement will be explained by the following.

4.1.1 Event Generation

W events are generated with ResBos [12] which models the W p_T spectrum. the g_2 parameter 2.3 which contributes to the W p_T spectrum is obtained after a fit of the CDF p_T spectrum: $g_2 = 0.685 \pm 0.048$ GeV^2
ResBos is coupled with WGRAD [41] which accounts for relevant QED processes. The major QED uncertainty is due to the fact that WGRAD does not include more than one final-state photon and that an ad-hoc correction based on [42] is applied.
The PDFs enter in the W mass uncertainty through their effects on the detector acceptance and kinematics on the decay charged leptons. W boson mass templates are generated with CTEQ6M PDFs. The systematic uncertainty due to PDFs is estimated from events generated in PYTHIA for each of the 20 CTEQ6 PDF uncertainty pairs [19].
Finally the total systematic uncertainty due to event generation is 11 MeV on the W boson mass for the M_T fit, 20 MeV on the lepton $p_T(l)$ fit and, 13 MeV on the $p_T(\nu)$ fit.

[5] $M_T = \sqrt{2p_T(l)p_T(\nu)[1-\cos(\phi_l - \phi_\nu)]}$

4.1.2 Momentum Scale Calibration

The momentum scale is extracted from the high statistics $J/\psi \to \mu\mu$ and $\Upsilon(1S) \to \mu\mu$ quarkonia decays and applied to the W and Z samples. The $Z \to \mu\mu$ sample is used to cross-check the scale and then combined with $J/\psi \to \mu\mu$ and $\Upsilon(1S)$ samples. Figure 13 shows the $Z \to \mu\mu$ mass fit which is in good agreement with the world-average Z mass. The resulting tracker momentum scale uncertainty is 17 MeV on the W mass.

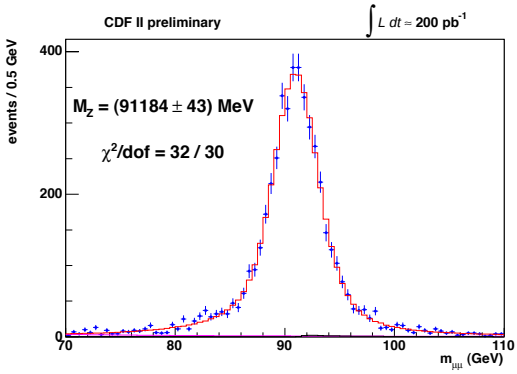

Figure 13: *The fitted $Z \to \mu\mu$ mass using the momentum scale derived from the $J/\psi \to \mu\mu$ and $\Upsilon(1S)$ calibration.*

4.1.3 Energy Scale calibration

The electromagnetic calorimeter energy scale is set using the peak of the E/p electron distribution (see Fig. 14) from $W \to e\nu$ events.
The $Z \to e^+e^-$ mass is then fitted to cross-check the energy scale and the non-linearity. Obtaining consistency, the measurement from E/p and the $Z \to e^+e^-$ mass are combined to obtain the most precise energy scale. The tail of the E/p (Fig. 14) distribution is fitted to tune the absolute number of radiation length in the tracker material. The uncertainty on this number of radiation length is then propagated to an uncertainty in the energy scale. The total uncertainty on the energy scale and non-linearity results in a W mass uncertainty of 30 MeV.

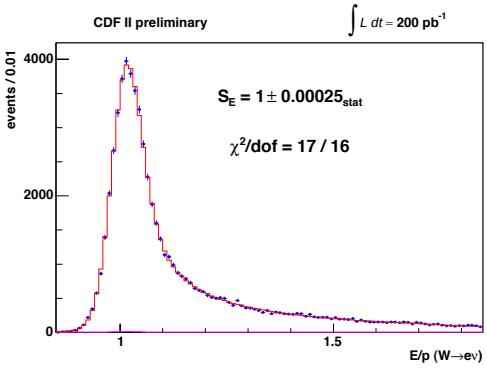

Figure 14: *The electron E/p distribution, modelled with the best-fit energy scale, material scale, and resolution.*

4.1.4 Recoil Calibration

Transverse recoil u_T is defined as all particles recoiling against the W or Z bosons. The $Z \to e^+e^-$ and $Z \to \mu^+\mu^-$ data are used to tune the recoil response and the resolution parameters. A combination of minimum bias data and $Z \to l^+l^-$ data is performed to describe the behavior of the hadronic recoil. Figure 15 shows that the model is reproducing well u_T distribution observed in the data.

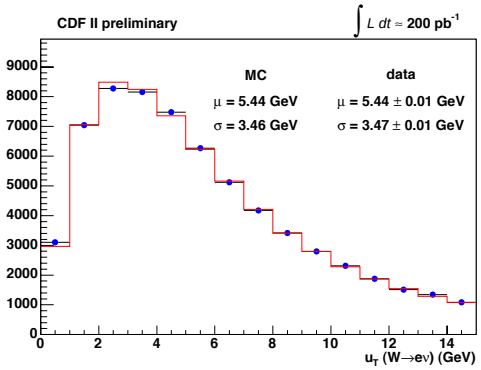

Figure 15: *The simulation (solid) and data (circles) u_T distributions for W boson decays to $e\nu$. The simulation uses parameters fit from Z boson data, and the uncertainty on the simulation is due to the statistical uncertainty on these parameters. The data mean (μ) and RMS (σ) aer well-modeled by the simulation.*

4.1.5 Mass Fit and Results

After background subtraction, the W mass is measured by performing a binned maximum-likelihood fit to lepton and neutrino (p_T),and transverse mass (M_T). Figure 16 and Fig. 17 show the mass fits for the transverse mass distribution in muon and electron sample respectively.

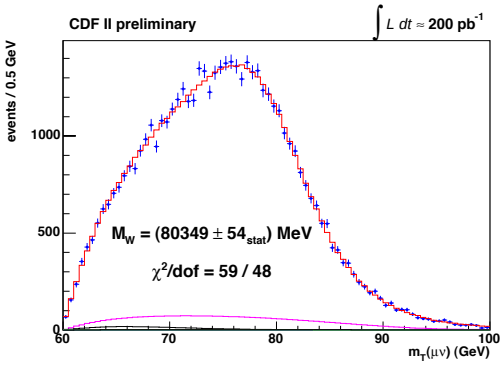

Figure 16: *The W boson transverse mass fits for the muon channel. The errors are statistical only*

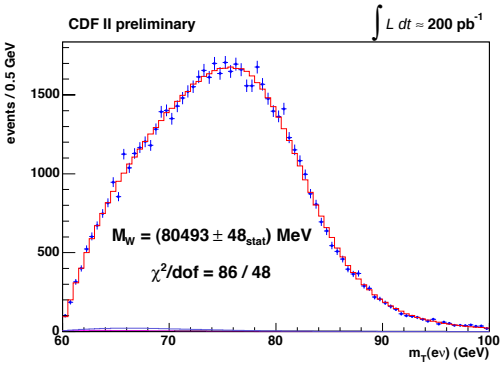

Figure 17: *The W boson transverse mass fits for the electron channel. The errors are statistical only*

Table 2 shows the systematic uncertainties for the transverse mass fits.

Systematics (MeV)	Electrons	Muons
Lepton Scale	30	17
Lepton Resolution	9	3
Recoil Scale	9	9
Recoil Resolution	7	7
Lepton ID	3	1
Lepton Removal	8	5
Backgrounds	8	9
p_T(W)	3	3
PDF	11	11
QED	11	12
Total	39	27

Table 2: *Table of systematics uncertainties for the transverse mass fits. The "Lepton Removal" uncertainty is due to the estimation of the fraction of the recoil in the lepton cluster.*

Finally the W boson mass from fits to the transverse mass, transverse momentum and transverse missing energy distributions are combined giving the single most precise M_W measurement [46, 47] to date:
$M_W = 80413 \pm 34(stat) \pm 34(syst)$ MeV
$= 80413 \pm 48$ MeV.
Figure 18 shows the W boson mass measurement at LEP and Tevatron experiments as well as the world average: $M_W = (80.398 \pm 0.025)$ GeV. The updated world average impacts the global precision elctroweak fits, reducing the preferred M_H by 6 GeV to 76^{+33}_{-24} GeV. The 95% C.L. upper limit on M_H is 144(182) GeV with(without) LEP II direct limit included [49].
With more statistics, both experiments CDF and DØ are looking forward to measuring the W boson mass with a precision of the order of 25 MeV per experiment.

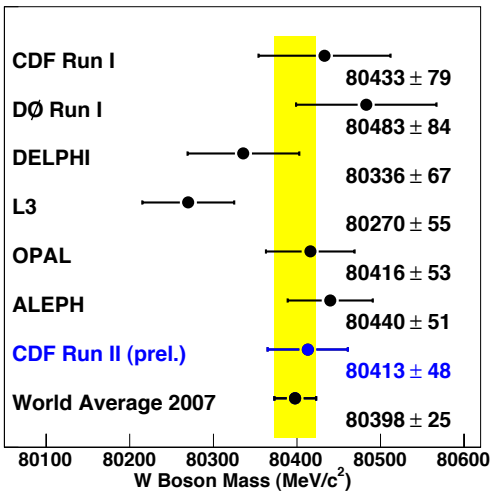

Figure 18: *W boson mass measurements at LEP and Tevatron and the world average value including the CDF Run II measurement*

4.2 W Boson Width Measurement

A precise measurement of width (Γ_W) provides a stringent test of SM prediction which is accurate to 2 MeV [48]. The first Run II preliminary result on Γ_W has been presented by DØ with an integrated luminosity of 177.3 pb^{-1}. The W direct width measurement was determined to be $\Gamma_W = 2.011 \pm 0.093(stat) \pm 0.107(syst)$ GeV. More recently CDF has performed a W direct width measurement with 350 pb^{-1} of data sample. The measurement is performed in the $e\nu$ and $\mu\nu$ decay channels.

The analysis is very similar to the W mass one. A Monte Carlo simulation is used to predict the M_T distribution as a function of Γ_W. Then these predictions are fitted to the data with a binned maximum-likelihood fit to extract Γ_W. While the fit for M_W is performed in the region around the peak of the distribution (65-90 GeV), the fit for Γ_W is performed in the high M_T tail region (90-200 GeV). This region is sensitive to the Breit-Wigner line-shape and less sensitive to the detector resolution as shown in Fig. 19.

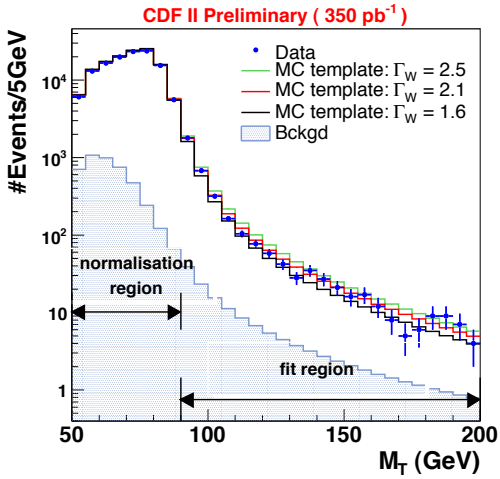

Figure 19: *Transverse mass spectra from the data and Monte Carlo simulation with different W widths showing the sensitivityy of the M_T tail region (90-200) GeV to the Breit-Wigner line-shape*

Table 3 shows the uncertainties on the W width measurement. As expected the tail region of m_T distribution is more sensitive to background and recoil resolution.

Systematics (MeV)	Electrons	Muons
Lepton Scale	21	17
Lepton Resolution	31	26
Simulation	13	
Recoil Scale	54	49
Lepton ID	10	7
Backgrounds	32	33
p_T(W)	7	7
PDF	16	17
QED	8	1
M_W	9	9
Total Systematic	78	70

Table 3: *Table of systematics uncertainties for the W width measurement. As expected the major uncertainties are due to the background and recoil*

Figure 20 shows the M_T fits for Γ_W in the muon and electron decay channels. The results are combined to give the final result $\Gamma_W = 2032 \pm 71$ MeV, the world's most precise single measurement.

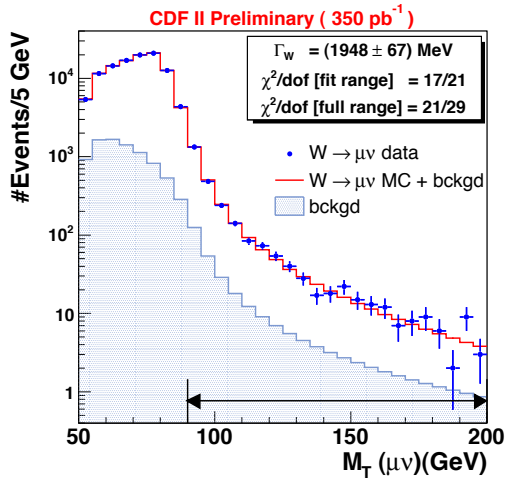

Figure 20: *Transverse mass fit for Γ_W measurement in $W \to \mu\nu$ decay channel*

This result, in good agreement with the SM prediction [48], reduces the world average central value as shown in Fig. 21, by 44 MeV and uncertainty by 22%.

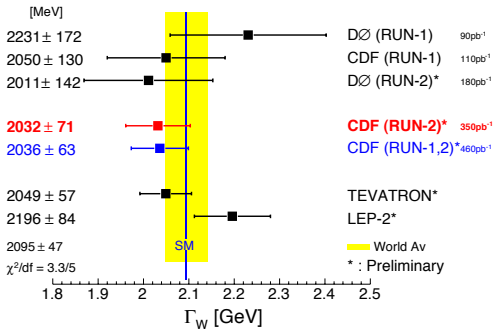

Figure 21: Γ_W *measurements at LEP [49] and at Tevatron experiments and the world combined value including this CDF measurement*

5 Conclusion

The analyses reported here are based on only a small fraction of the expected data. There is significant room for improving the precision of current measurement with around 8 fb^{-1} data sample expected at the completion of the Tevatron. Nevertheless, the large sample analysed up to now accommodate a wide variety of electroweak measurements. The WW production has been observed at 6σ while the ZZ production has been observed at 3σ. The precision of many measurements at Tevatron is now surpassing LEP *e.g*, ZZγ anomalous TGC limits, M_W and Γ_W, and will continue to improve as datasets will grow by up a factor ≈ 10. Future prospects in W mass measurement (≈ 25 MeV by experiment) will further constrain the Higgs mass [50] as shown in Fig. 22.

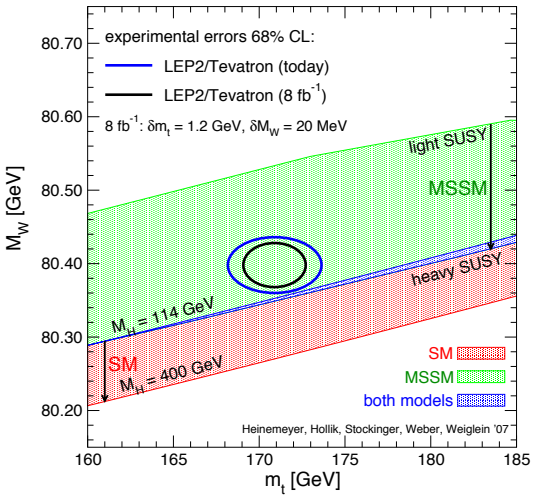

Figure 22: *Projection for the Tevatron constraints on M_H based on thye expected precision of combined top quark and W boson mass measurement assuming 8 fb^{-1} of data callected be each experiment*

6 Acknowledgements

It is a pleasure to thank my CDF and DØ colleagues for the exciting and fruitful collaboration, and our Tevatron colleagues for the excellent luminosity. I also thank very warmly the organisers for the very nice and interesting LP07 conference.

References

[1] CDF Collaboration, A. Abulencia *et al.*, Phys. Rev. D **75**, 092004 (2007).

[2] DØ Collaboration, B. Abbott *et al.*, Phys. Rev. D **71**, 072004 (2005).

[3] R.hamberg, W.L. van Neerven and T. Matsuura, Nucl. Phys. B359, 343 (1991).

[4] DØ Collaboration Phys. Rev. D **76** 012003 (2007).

[5] C. Anastasiou, L. Dixon, K. Melnikov and F. Petriello, Phys. Rev. D **69**, 094008 (2004).

[6] A. D. Martin, R. G. Roberts, W. J. Stirling and R. S. Thorne, Phys. Lett. B **604**, 61 (2004).

[7] J. Pumplin, D.R. Stump, J. Huston, H.L. Lal, P.Nadolksy, W.K. Tung, JHEP 0207 (2002).

[8] K. Melnikov, F. Petriello, Phys. Rev. D **74** 114017 (2006).

[9] J. Collins, D. Soper, G. Sterman, Nucl. Phys. **B250** (1985) 1999.
P.B. Arnold and R. Kauffman, Nucl. Phys. **B349**, 381 (1991).

[10] CDF Collaboration, T. Affolder *et al.*, Phys. Rev. Lett. **84**, 845 (2000).

[11] DØ Collaboration, B. Abbott *et al.*, Phys. Rev. D **61**, 032004 (2000); DØ Collaboration, B. Abbott *et al.*, Phys. Rev. Lett. **84**, 2792 (2000).

[12] C. Balazs, C.P. Yuan, Phys. Rev. D **56**, 5558 (1997).

[13] E. Barberio and Z. Was, PHOTOS: A Universal Monte Carlo for QED radiative corrections. Version 2.0 Comput. Phys. Commun 79, 291 (1994).

[14] F. Landry, R. Brock, P. Nadolsky, C.P. Yaun, Phys. Rev. D **67**, 073016 (2003).

[15] CDF Collaboration, D. Acosta *et al.*, Phys. Rev. D **71**, 051104 (2005).

[16] DØ Collaboration, V.M. Abazov *et al.*, hep-ex/0709.4254v1, submitted to Phys. Rev. R.C.

[17] C. Anastasiou *et al.*, Phys. Rev. **D69**, 094008 (2004).

[18] A.D. Martin *et al.*, Eur. Phys. J., **C28**, 455 (2003).

[19] J. Pumplin *et al.*, "New generation of parton distributions with uncertainties from global QCD analysis", hep-ph/0201195.

[20] CDF Collaboration, T. Affolder *et al.*, Phys. Rev. Lett. **94**, 041803 (2005).

[21] DØ Collaboration, B. Abbott *et al.*, Phys. Rev. D **71**, 091108 (2005).

[22] LEP Collaborations, Physics Report Volume 427 (2006).

[23] CDF Collaboration, D. Acosta *et al.*, Phys. Rev. Lett. **94**, 041803 (2005).

[24] DØ Collaboration, V.M. Abazov *et al.*, Phys. Rev. D **71**, 091108 (2005).

[25] U. Baur, S. Errede, and G. Landsberg, Phys. Rev. D **50**, 1917 (1994).

[26] D. Choundhury *et al.*, Int. J. Mod. Phys. A **16**, 4891 (2001).

[27] G.J. Gounaris, J. Layssac, and F.M. Renard, Phys. Rev. D **67**, 013012 (2003).

[28] DØ Collaboration, V.M. Abazov *et al.*, Phys. Rev. Lett. **95**, 051802 (2005).

[29] W.-M. Yao *et al.*, J. Phys. G: Nucl. Part. Phys. **33** (2006).

[30] U. Baur, T. Han, and J. Ohnemus, Phys.Rev. D **57**, 2823 (1998).

[31] DØ Collaboration, V.M. Abazov *et al.*, Phys. Lett. B 653, 378 (2007).

[32] U. Bauer and E. Berger, Phys. Rev. D **47**, 4889 (1993).

[33] M.S. Neubauer, for the CDF and DØ collaborations, hep-ex/0605066 (2006).
CDF Collaboration, D. Acosta *et al.*, Phys. Rev. Lett. **94**, 211801 (2005).

[34] DØ Collaboration, V. M. Abazov *et al.*, Phys. Rev. Lett. **94**, 151801 (2005).

[35] J.M. Campbell and R.K. Ellis, Phys. Rev. D **60**, 113006 (1999).

[36] CDF Collaboration, A. Abulencia *et al.*, Phys. Rev. Lett. **98**, 161801 (2007).

[37] K. Hagiwara, R.D. Peccei, D. Zeppenfeld, annd K. Hikasa, Nucl. Phys. **B282**, 252 (1987).

[38] K. Hagiwara, S. Ishihara, R. Szalapski, and D. Zeppenfeld, Phes. Rev. D **48**, 2182 (1993).

[39] CDF Collaboration, F. Abe *et al.*, Phys. Rev. Lett. **78**, 4536 (1997).
DØ Collaboration, V. M. Abbott *et al.*, Phys. Rev. D. **60**, 072002 (1999).
LEP Collaborations ALEPH, DELPHI, L3, OPAL,and LEP TGC Working Group, Report No. LEPWWG/TGC/2005-01 (2005).
DØ Collaboration, V. M. Abazov *et al.*, Phys. Rev D **74**, 057101 (2006).

[40] DØ Collaboration, V. M. Abazov *et al.*, hep-ex/0709.2917 submitted to Phys. Rev. D R.C.

[41] U. Baur, S. Keller, and D. Wackeroth, Phys. Rev. D **59**, 013002 (1998).

[42] C.M. Carloni Calame *et al.*, Phys. Rev. D **69**, 037301 (2004).

[43] W.J.Marciano, Phys. Rev. D **20**, 274 (1979); F. Antonelli, M. Consoli, and G. Corbo, Phys. Lett. B **91**, 90 (1980); M. Veltman, *ibid.*, 95 (1980).

[44] A. Stirlin, Phys. Rev. D **22**, 971 (1980).

[45] CDF and DØ Collaborations (combined top mass result) hep-ex/0703034 (2007).

[46] CDF Collaboration, T. Aaltonen *et al.*, hep-ex/0707.0085, submitted to Phys. Rev. Lett.

[47] CDF Collaboration, T. Aaltonen *et al.*, hep-ex/0708.3642, submitted to Phys. Rev. D

[48] W.M. Yao *et al.*, J. Phys. G **33** (2006).

[49] LEP Collaborations and LEP Electroweak Working Group, http://lepewwg.web.cern.ch/LEPEWWG/, hep-ex/0612034.

[50] S. Heinemeyer, W. Hollik, D. Stockinger, A.M. Weber and, G. Weiglein, hep-ph/0604147